Transition Radiation Spectra of Electrons from 1 to 10 GeV/c in Regular and Irregular Radiators

A. Andronic [a], H. Appelshäuser [b], R. Bailhache [a], C. Baumann [c],
P. Braun-Munzinger [a], D. Bucher [c], O. Busch [a], V. Cătănescu [d],
S. Chernenko [e], P. Christakoglou [f], O. Fateev [e], S. Freuen [g],
C. Garabatos [a], H. Gottschlag [c], T. Gunji [h], H. Hamagaki [h],
N. Herrmann [g], M. Hoppe [c], V. Lindenstruth [i], C. Lippmann [a,*],
Y. Morino [h], Yu. Panebratsev [e], A. Petridis [f], M. Petrovici [d],
I. Rusanov [g], A. Sandoval [a], S. Saito [h], R. Schicker [g], H.K. Soltveit [g],
J. Stachel [g], H. Stelzer [a], M. Vassiliou [f], B. Vulpescu [g], J.P. Wessels [c],
A. Wilk [c], V. Yurevich [e], Yu. Zanevsky [e]

for the ALICE collaboration.

[a] *GSI Darmstadt (Germany)*
[b] *Institut für Kernphysik, University of Frankfurt (Germany)*
[c] *Institut für Kernphysik, University of Münster (Germany)*
[d] *NIPNE Bucharest (Romania)*
[e] *JINR Dubna (Russia)*
[f] *University of Athens (Greece)*
[g] *Physikalisches Institut, University of Heidelberg (Germany)*
[h] *University of Tokyo (Japan)*
[i] *Kirchhoff-Institut für Physik, University of Heidelberg (Germany)*

Abstract

We present measurements of the spectral distribution of transition radiation generated by electrons of momentum 1 to 10 GeV/c in different radiator types. We investigate periodic foil radiators and irregular foam and fiber materials. The transition radiation photons are detected by prototypes of the drift chambers to be used in the Transition Radiation Detector (TRD) of the ALICE experiment at CERN, which are filled with a Xe, CO_2 (15 %) mixture. The measurements are compared to simulations in order to enhance the quantitative understanding of transition radiation production, in particular the momentum dependence of the transition radiation yield.

Key words: TRD, transition radiation spectra, foil radiator, foam radiator, fiber radiator,

1 Introduction

The ALICE Transition Radiation Detector (TRD) [1,2] is a large area (750 m^2, 1.18 million readout channels) device that offers precise tracking and electron identification and – combining these two capabilities – a fast trigger on high-p_t electrons and jets. The readout chambers are drift chambers with a 3 cm drift region and a 0.7 cm amplification region, separated by a cathode wire grid. They are read out by cathode pads of varying sizes via charge sensitive preamplifiers/shapers (PASA). The maximum drift time is about 2 μs and the induced signal is sampled on all channels at 10 MHz to record the time evolution of the signal [3,4]. A *sandwich* radiator is placed in front of each gas volume, which is a box structure of foam (*Rohacell HF71*, 8 mm), reinforced by a carbon fiber laminate coating on both sides and containing seven layers of polypropylene fiber sheets (*Freudenberg LRP375BK*, 5 mm each). A drift cathode made of 12 μm aluminized mylar is laminated onto the carbon fiber. This design was chosen in order to find a compromise between maximum transition radiation yield and a solid construction for our large area detectors.

Transition radiation (TR) is emitted by particles traversing the radiator with a velocity larger than a certain threshold [5], which corresponds to a Lorentz factor of $\gamma \approx 1000$. The produced TR photons have energies in the X-ray range, with the bulk of the spectrum from 1 to 30 keV. In the drift chambers of the ALICE TRD a gas mixture of Xe and CO_2 (15 %) is used to provide efficient absorption of these photons. To discriminate electrons from the large background of pions in the momentum range of interest (1 to 10 GeV/c), two characteristic phenomena are used [6]:

i) The ionization energy loss [7] is larger for electrons than for pions, since electrons are at the plateau of ionization energy loss, while pions are minimum ionizing or in the regime of the relativistic rise.
ii) Only electrons reach a velocity that exceeds the TR production threshold.

In the ALICE TRD, as in any other TRD, TR is superimposed on the ionization energy loss, due to the small angle of emission ($\backsim 1/\gamma$) with respect to the emitting particles trajectory. This explains why the existing measurements of TR spectra [8,9,10,11] are scarce. In this publication, we investigate specific features of TR,

---
* Corresponding author
   Email address: `C.Lippmann@gsi.de` (C. Lippmann).
   URL: `http://www-linux.gsi.de/~lippmann` (C. Lippmann).

in particular its spectral distributions and momentum dependence produced in the ALICE TRD *sandwich* radiators. By improving the experimental setup with respect to a similar earlier measurement [8], we are able to cover the full momentum range from 1 to 10 GeV/c. In addition, we also investigate different irregular radiators and two regular foil radiators.
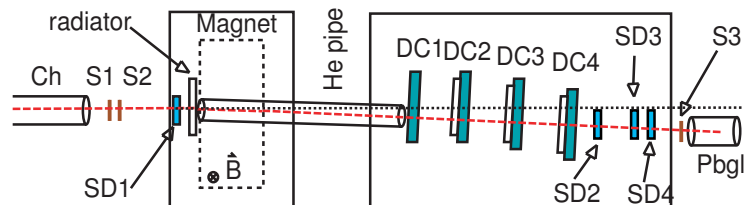
2   Experimental Setup and Analysis Method

Fig. 1. Setup of the beam test. A radiator is placed in front of the dipole magnet, which separates the beam from the TR photons produced in the radiator. A pipe filled with helium is used to minimize the absorption of the TR photons on the ∼1.6 m long path to the drift chamber (DC1). Three other drift chambers (DC2-DC4) have a radiator in front and are used for reference and for dE/dx measurements. Electrons can be selected by coincident thresholds on a Čerenkov detector (Ch) and a lead-glass calorimeter (Pbgl). Three scintillating detectors (S1-S3) are used for triggering and four silicon detectors (SD1-SD4) for position reference.

The measurements were carried out at the T9 secondary beam line at the CERN PS accelerator. The beam consisted of electrons and pions with momenta of 1 to 10 GeV/c. The method to study TR is similar to that described in [9]; a sketch of our setup is shown in Fig. 1. A dipole magnet is used to deflect the beam in order to spatially separate the TR photons from the path of the beam (see Fig. 3). A 1.6 m long pipe filled with helium is used to minimize photon absorption. The photons also have to cross the two entrance windows to the helium pipe (20 μm mylar foil each), a small amount of air (≈1 mm on both sides) and the entrance window (drift cathode) of the prototype drift chamber (20 μm mylar foil with aluminium sputtering, ≈1 μm). The length of the magnet is approximately 0.5 m. The radius of a beam particle is kept approximately constant (33 m) for the different momenta by adjusting the strength of the magnetic field up to about 1 T at 10 GeV/c.

The parameters of all radiators investigated in this work are given in table 1. The *foam* and *fiber* radiators are each made of the same materials which are components of the ALICE TRD *sandwich* (see Fig. 2). The dummy radiator is made of plexiglas.

We use four identical prototype drift chambers with a geometry similar to that of the final TRD chambers, but with a smaller active area (25×32 cm^2). The dimensions of the pads are 0.75×8 cm^2. We use the final version of the ALICE TRD
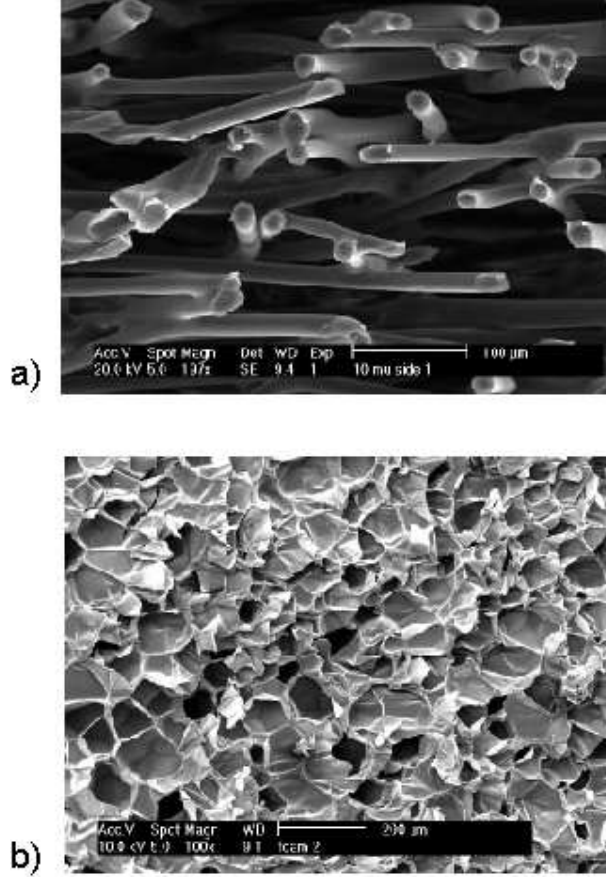
Fig. 2. SEM pictures of the irregular radiator materials: Polypropylene fibers (*Freudenberg LRP375BK*) (a) and *Rohacell* foam (HF71) (b).

	thickness [cm]	N_f [ ]	d_1 [μm]	d_2 [μm]	density [g/cm^3]	X/X_0 [%]
Sandwich	4.8	(115)	(13)	(400)	-	0.87
Fiber	4.0	(115)	(13)	(400)	0.074	0.65
Foam	4.2	-	-	-	0.075	0.78
Reg1	6.24	120	20	500	-	0.61
Reg2	5.94	220	20	250	-	1.37
Dummy	0.4	-	-	-	1.18	1.2

Table 1
Properties of the various radiators investigated. N_f and d_1 are the number and thickness of the foils, d_2 is the spacing. For the *sandwich* and *fibers* radiator the numbers used as parameters in the simulation are given in parenthesis.

PASA with an on-detector noise of about 1000 electrons (r.m.s.). The drift chambers are read out with a Flash ADC system at 20 MHz, which is twice the nominal sampling rate of the TRD, to increase the position resolution in the drift direction. The high voltage at the anode wires is adjusted to provide a relatively low gas
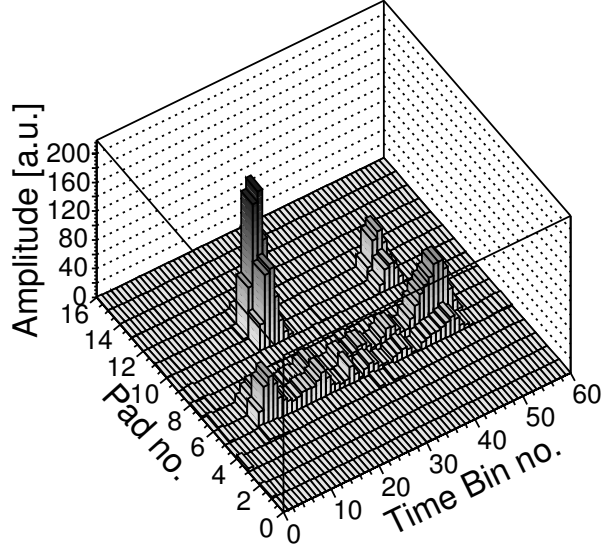
Fig. 3. Pulse height versus drift time on sixteen adjacent cathode pads for an example event. The maximum drift time at the electron drift velocity of 1.5 cm/μs is about 2 μs, thus at the employed sampling frequency of 20 MHz one time bin corresponds to about 0.75 mm in the drift direction perpendicular to the wire planes. The time zero is arbitrarily shifted by 0.5 μs to facilitate a simultaneous measurement of the baseline and of noise. The baseline is subtracted in the shown event. Here, the ionization signal by a beam electron and two well separated photon clusters are clearly visible.

gain (around 4000) to minimize space charge effects [12]. A few presamples are taken for each channel in order to extract information on the baseline and noise. The signal generated by the ionization energy loss and by the TR photons is measured simultaneously on a row of 16 readout pads. An example event is shown in Fig. 3. For each event a TR cluster search is performed. We are able to provide a separation from the beam of more than three pads at all momenta, which avoids a contamination of the measured TR energy with ionization energy. The obtained charge spectra are calibrated using the 5.96 keV line of ^{55}Fe [7] and by comparing the most probable pion energy loss in the TRD chambers to earlier measurements and to simulations (including corrections for ambient variations).

3 Transition Radiation and Detector Performance Simulations

In general, all ALICE related simulations are carried out using AliRoot [13], the ALICE software package. The interaction of the charged particles with the detector materials and their energy loss are currently simulated using Geant 3.21 [14]. In principle the employed "Virtual Monte Carlo" would allow one to run also different simulation engines (Geant 4 [15] or Fluka [16]) without changing the user code containing the input and output format nor the geometry and detector response definition.

For the simulation of the performance of the TRD detector system a quantitative understanding of TR is indispensable. Since the production of TR is not included in Geant 3, we have explicitly added it to AliRoot. We use an approximation for the TR yield of a regular stack of foils with fixed thickness, including absorption [9], which we tune to reproduce the measured performance of the irregular ALICE TRD radiators [6,8]. Geant 4 is in principle able to simulate the TR emitted by regular and irregular structures [17]. A satisfactory comparison to our measured data has however not been accomplished yet.
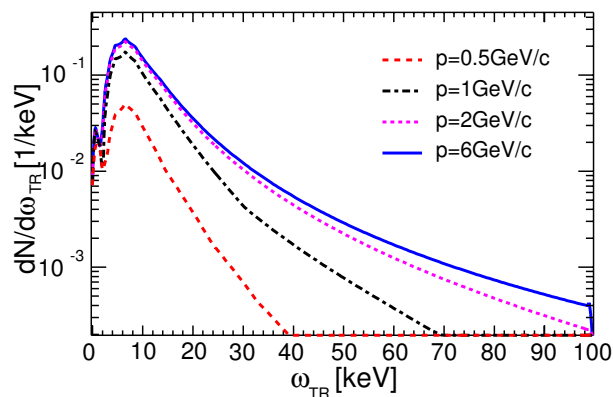

Fig. 4. Calculated TR spectra at the end of a regular radiator with $N_f = 220$, $d_1 = 20\,\mu$m and $d_2 = 250\,\mu$m (*Reg2*) for electrons at four momenta. We find $\langle N_{TR}^{prod}\rangle$=0.46, 1.68, 2.41 and 2.63 for electrons at $p = 0.5$, 1, 2 and 6 GeV/c, respectively. The distributions are obtained using the formalism of Ref. [9].

A formula for the energy spectrum of the TR photons emitted by a highly relativistic electron passing through a radiator composed of N_f foils of thickness d_1, spaced periodically by gaps of width d_2, has been given in [9]. Some example spectra of the energy of TR photons exiting a regular radiator calculated using that formula are shown in Fig. 4. The onset of TR production takes place around 0.5 GeV/c and the predicted TR yield essentially saturates above 2 GeV/c. The average number $\langle N_{TR}^{prod}\rangle$ of produced TR photons per electron event is given by the integral of these spectra. To simulate the emission and detection of TR photons we proceed in three steps:

(1) Draw a number from a Poisson distribution with a mean given by $\langle N_{TR}^{prod}\rangle$,
(2) calculate the energies of these produced photons by drawing a random number from the differential energy spectrum (Fig. 4) and
(3) propagate these photons through the experimental setup.

All materials crossed by the photons, e.g. gas volumes and foil windows are taken into account by including the energy dependent absorption lengths of the given materials in the simulation. We use tabulated X-ray mass attenuation coefficients from Ref. [19]. The detector energy resolution of 32 % (σ), as measured with a ^{55}Fe source, is folded in.

4 Results

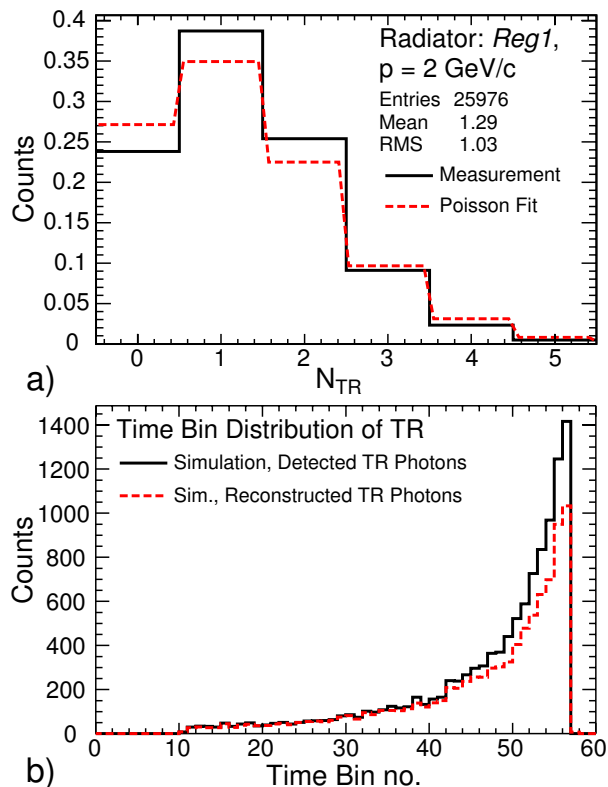## 4.1 Cluster Number Distribution

Fig. 5. a) Photon number distribution for 2 GeV/c beam momentum for the radiator *Reg1* together with a Poisson fit. b) Simulated time bin distributions for the absorption of TR photons.

In Fig. 5a we present the distribution of the detected number of photons per incident electron for 2 GeV/c electrons for the radiator *Reg1*. The shape of the distribution can be approximated by a Poissonian, indicated by the dashed histogram. The minimum time interval between two TR photons resolved by the algorithm is given by two time bins (100 ns), corresponding to about 1.5 mm. This can lead to a considerable amount of events with overlapping clusters. Fig. 5b shows for simulated events the time bin distribution of the detected TR clusters and of the clusters reconstructed by the TR search algorithm. Close to the drift cathode (for large time bin numbers) the density of the TR hits is largest and, as a consequence, the probability to misidentify two close photon events to be a single TR photon one is highest in this region.
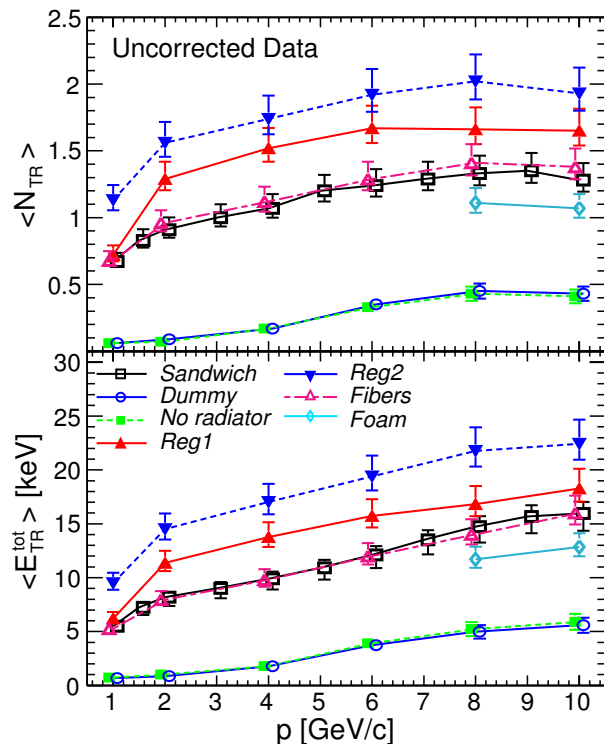
Fig. 6. Measured momentum dependence of the mean number of reconstructed TR photons (upper panel) and of the mean total TR energy measured as a function of momentum (lower panel).

While for our earlier measurement of TR spectra the range in momenta covered was restricted by the possible range of the magnetic field and by the experimental configuration [8], we are now able to present measurements over a broad momentum range from 1 to 10 GeV/c. The (uncorrected) results for all radiators are shown in Fig. 6. Here $\langle N_{TR} \rangle$ denotes the mean number of detected TR clusters and $\langle E_{TR}^{tot} \rangle$ is the mean energy deposited in the detector by TR by one electron. The energy threshold of the TR cluster search algorithm is about 0.1 keV. For all radiators, a systematic increase of the photon yield as a function of momentum is observed. The two regular radiators show the best performance, followed by the *fiber* radiator and the *sandwich*. For the *foam* radiator only two measurements at 8 and 10 GeV/c are available; the photon yield of this material is somewhat lower than for the other cases. With the *dummy* radiator and without radiator we observe a considerable amount of photons in the drift chamber. This photon background is investigated in the following section.

4.3   Photon Background

TR from our radiators is not the only possible source of photons detected in the drift chamber. One could suspect TR from different sources (material in the beam line), bremsstrahlung from material in the beam (or from the radiators) and synchrotron radiation from the electrons in the magnetic field. The influence of bremsstrahlung created in the radiators can be investigated by looking at the data for the dummy radiator (since its radiation length is comparable to the radiation length of the radiators, see Table 1) and comparing it to the data without radiator (see Fig. 6). Since the photon yield is very similar, we can exclude that the influence of bremsstrahlung from the radiators is significant.
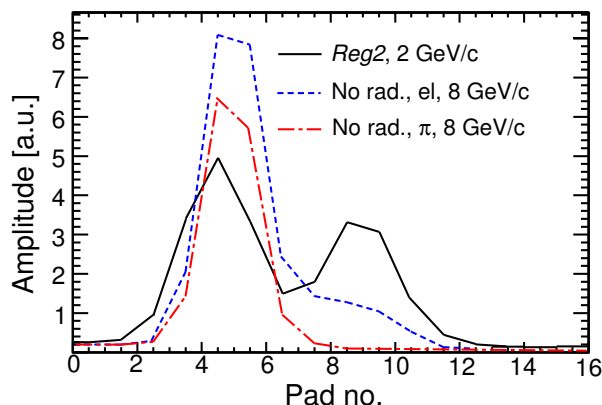

Fig. 7. Example distributions of the average signal amplitudes on the 16 readout pads. We compare a run with the *Reg2* radiator to a run without radiator. The peak around pad numbers 4 and 5 corresponds to the position of the beam. Distributions to the right of these peaks indicate charge deposit by photons (TR and/or SR).

While the contribution of TR from other material in the beam line is expected to be very small, the production of synchrotron radiation (SR) can be significant. This explanation is supported by the distribution of the average signal amplitudes across the pads shown in Fig. 7. For pions the only contribution is the ionization energy deposit. For electrons, the contribution of TR is well separated from the ionization energy deposit. On the other hand, the distribution of deposited energy for electrons at high momenta and without a radiator shows a shape that corresponds to what is expected from SR. In this case SR photons are emitted continuously along the curved electron tracks and their absorption with respect to the beam position in the detector is expected to be uniform up to a certain distance from the particle track.

4.4   Simulation of Synchrotron Radiation

Synchrotron radiation (SR) occurs when charged particles move on a curved path. Since the energy radiated by the particle is proportional to γ^4, it can be produced

with a sizeable yield in our momentum range by electrons only. In the following treatment, the magnetic field is assumed to be constant and uniform, neglecting possible fringe field effects. Then the energy radiated by an ultra-relativistic electron along a trajectory of length L is [18]

$$\Delta E_{SR} = \frac{2}{3} \frac{L}{R^2} \frac{e^2}{4\pi\varepsilon_0} \beta \gamma^4 \quad (\text{for} \quad L \ll R).$$ (1)

The velocity β of the particle is measured in units of the speed of light. We are interested in the spectral distribution of the radiated photons $\frac{dN}{d\omega_{SR}}$. This can be expressed in terms of the mean energy loss spectrum

$$\frac{dN}{d\omega_{SR}} = \frac{\sqrt{3}}{2\pi} \alpha \frac{L\gamma}{R} \frac{1}{\omega_C} \int\limits_{\omega_{SR}/\omega_C}^{\infty} K_{5/3}(\eta)\, d\eta,$$ (2)
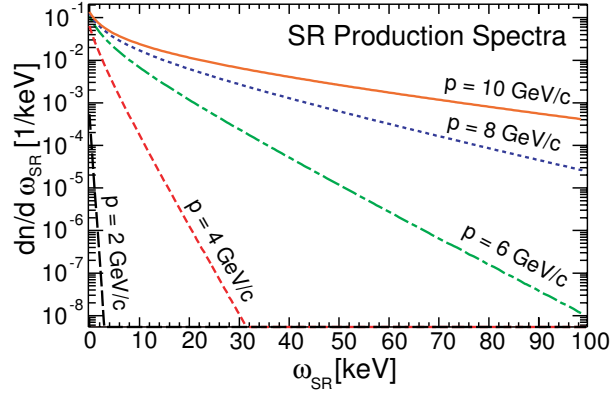

Fig. 8. Synchrotron Radiation (SR) production spectra as calculated using Eq. 2 for electrons at five momenta, $L = 0.5\,\mathrm{m}$, $R = 33\,\mathrm{m}$.

with ω_{SR} the synchrotron photon energy, α the fine structure constant and $K_{5/3}$ the MacDonald function[1]. The characteristic energy ω_C of the SR is given by $1.5 \frac{\beta\hbar c}{R} \gamma^3$. Examples of SR energy spectra are shown in Fig. 8. The mean number of produced SR photons at all energies is the integral of the spectral distribution (Eq. 2), which can be approximated as

$$\langle N_{SR}^{prod} \rangle \approx 10^{-2} \frac{L\gamma}{R}.$$ (3)

Fig. 9 shows the measured photon background from Fig. 6 (without radiator) together with SR simulations. The mean number of SR photons produced per electron along the curved electron track is about 0.4 at 1 GeV/c and rises to around 4

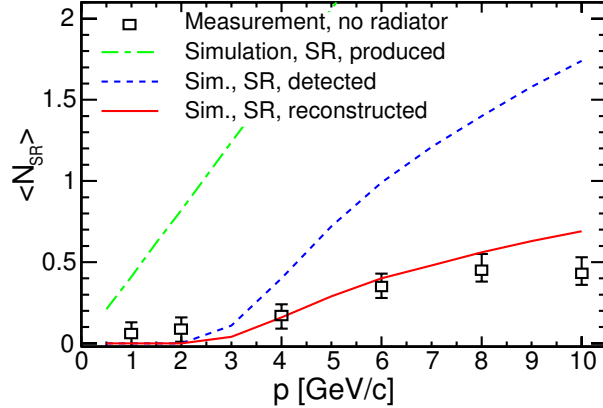[1] The modified Bessel function of the second kind.

Fig. 9. Measured number of detected photons without radiator as a function of the beam momentum together with simulations for synchrotron radiation (SR).

at 10 GeV/c. However, most low energy photons are absorbed in the material before the drift chamber volume, while at higher momenta some high energy photons ($\gtrsim$30 keV) exit the drift chamber undetected. As a consequence, we find that no photons are detected up to 2 GeV/c electron momentum and about 1.7 at 10 GeV/c. The cluster search algorithm is not able to reconstruct photons that are deposited very close to the beam, where a large part of the SR photons are expected to be deposited. By running the cluster search algorithm on simulated SR data we observe a reconstruction efficiency of around 40 %. Taking this into account, the agreement with the measurement is very good and we conclude that we observe a background of synchrotron radiation in our measurements. This background can be subtracted when investigating mean values. In addition, in the momentum region up to 2 GeV/c the contribution of SR is negligible, and as a consequence our TR energy spectra for those momenta are free from SR. Fig. 10 shows measured photon energy spectra without radiator together with simulated SR spectra for electrons of 6 GeV/c. The agreement is quite good.

4.5 TR Spectra

In this section we compare the measured spectral distributions of TR for 2 GeV/c electrons to simulations. The low energy threshold of the TR search algorithm (0.1 keV) and the dynamic range of the employed Flash ADC system lead to meaningful data in the energy range of interest.

In Fig. 11 we show the measured distributions of TR energy per photon (E_{TR}) and per incident electron (total TR energy, E_{TR}^{tot}) for the two regular radiators at 2 GeV/c together with simulations. The simulated spectra are obtained using the procedure described in section 3, where the values of N_f, d_1 and d_2 are fixed by the geometries of the radiators (see table 1). If a correction for the cluster separation inefficiency
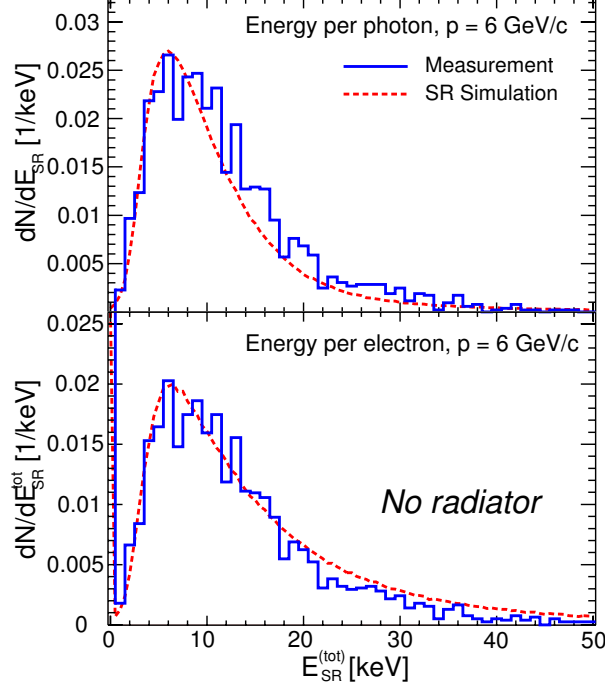
Fig. 10. Measured photon energy spectra without radiator together with simulated SR spectra at 6 GeV/c. The upper panel shows the distribution of the energy for single photons. Here the simulated spectrum is scaled down by a factor of 0.4 to account for the photon detection efficiency of the algorithm due to the overlap of the photon absorption with the energy deposit from the beam particles. The lower panel shows the distribution of the total SR energy. The entries in the bin at 0 keV (off scale) correspond to events when no photon was detected.

is performed the agreement is good. However, the simulated spectra are somewhat harder in both cases.

The observable E_{TR}^{tot} is not affected by the TR search algorithm. Events with $E_{TR}^{tot} = 0$ are mainly due to events with no TR photon ($N_{TR} = 0$). Again, we observe that the simulated spectra are harder, especially for the radiator *Reg2*. This discrepancy can not be explained by slight variations of the foil number, thickness or spacing.

Measured and simulated TR spectra for the ALICE TRD *sandwich* radiator and for the *fiber* radiator at 2 GeV/c are shown in Fig. 12. The spectra for the two radiators are very similar, which is surprising, since the *sandwich* radiator also contains the carbon fiber and mylar layers and some amount of epoxy. In the simulation we use the theory described in section 3. Since the two radiators are not regular foil structures, the parameters N_f, d_1 and d_2 can only reflect typical dimensions of the radiator materials (see Fig. 2), but are not unambiguously determined. Our set of parameters ($N_f = 115$, $d_1 = 13\,\mu$m and $d_2 = 400\,\mu$m) was chosen to best reproduce our measurements, taking into account also the influence for the limited cluster separation efficiency. This set of parameters leads to a good agreement with
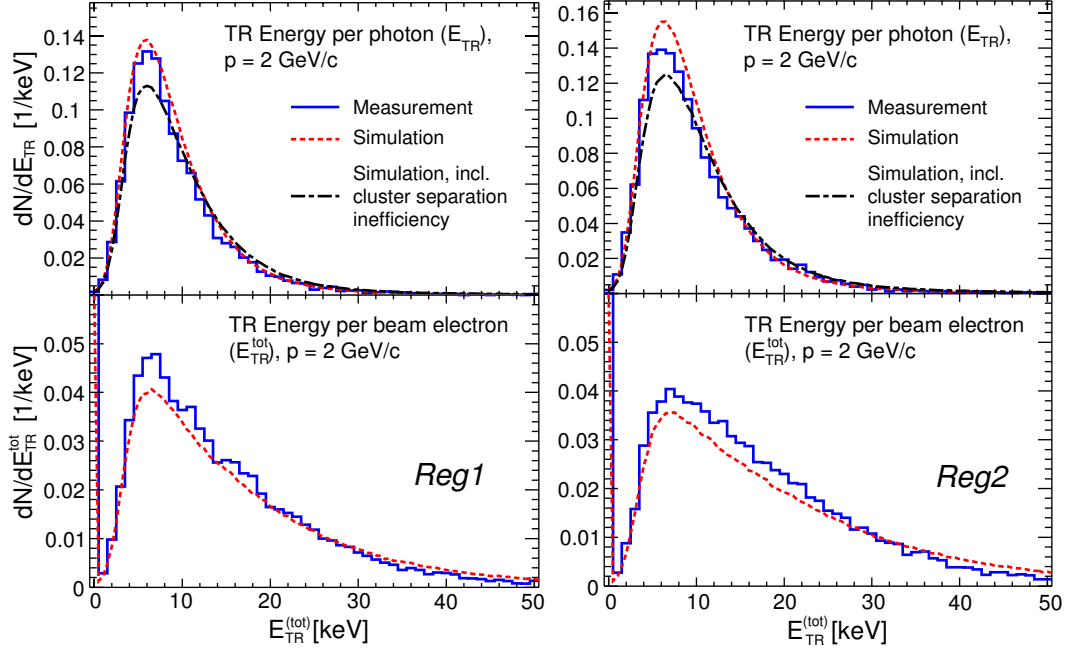
12

Fig. 11. Measured and simulated TR spectra at 2 GeV/c for the two regular foil radiators *Reg1* (left panels) and *Reg2* (right panels). The upper panels show the distribution of the energy for single TR photons. The lower panels show the distribution of the total TR energy detected per incident beam electron. The entries at 0 keV (off scale) correspond to events when no photon was detected.
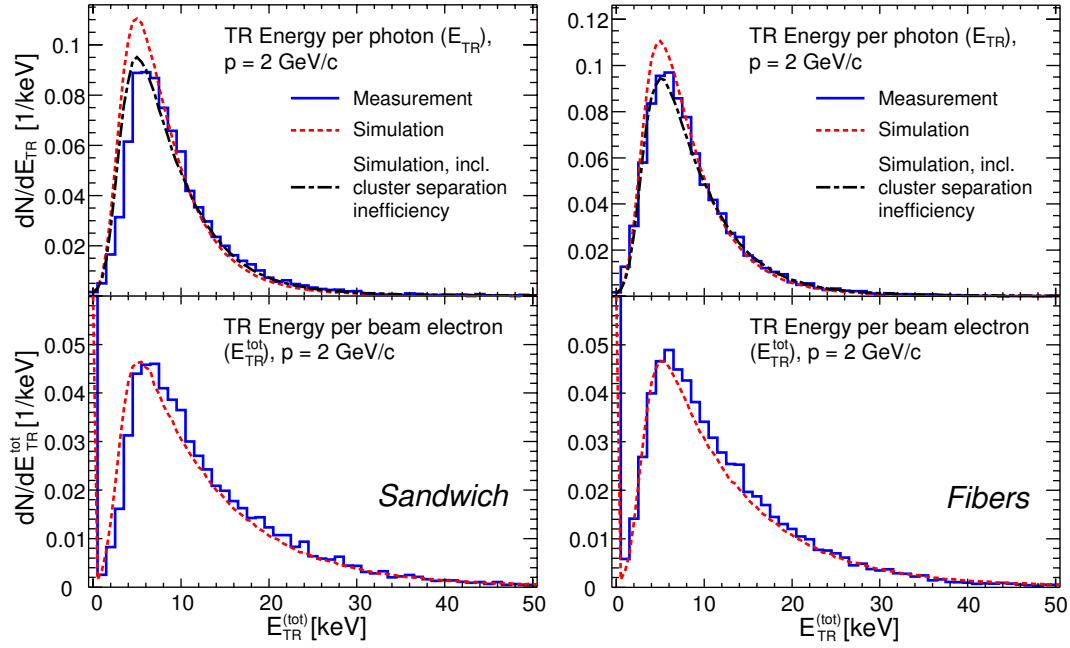

Fig. 12. Measured and simulated TR spectra at 2 GeV/c for the ALICE TRD *sandwich* radiator (left panels) and for the *fiber* radiator (right panels).

the data for both radiator types.

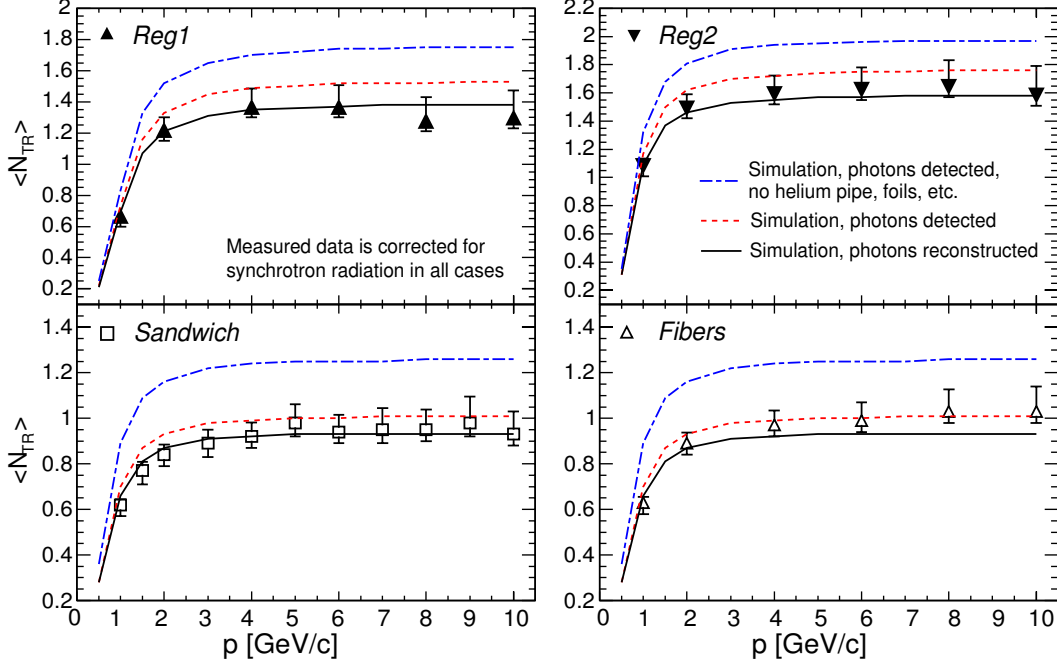## 4.6 Data Corrected for Synchrotron Radiation

Fig. 13. Measured and simulated dependence of the mean number of detected TR photons $\langle N_{TR} \rangle$ on the momentum for the two regular radiators and for the *sandwich* and *fiber* radiators. The measured data are corrected for SR; the simulated data show the actual detected mean number of TR photons with and without the helium pipe and its entrance windows included in the simulation and the mean number of photons reconstructed by the TR cluster search algorithm.

We perform the correction of the measured mean values of the TR yield for the photon background due to SR by subtracting the mean values obtained without radiator. Since we performed measurements for the *sandwich* radiator at more momenta than without radiator, the data at these momenta are obtained by the subtracting interpolated values for the SR background. Fig. 13 shows the momentum dependence of the mean number of TR photons $\langle N_{TR} \rangle$ for the two regular radiators, for the *sandwich* radiator and for the *fiber* radiator. We find that for all radiators up to roughly 0.2 photons are absorbed in the helium pipe, the entrance windows and the air in between. We also include in the simulation the full TR cluster search algorithm that was used on the measured data. This leads to a good reproduction of the measured data for the two regular radiators, in contrast to earlier findings, where the simulations overestimated the data, in particular for Xe-based detectors [10,11]. As already mentioned, in the case of the irregular radiators the parameters for the simulation (N_f, d_1 and d_2) were tuned to best reproduce the measurements.
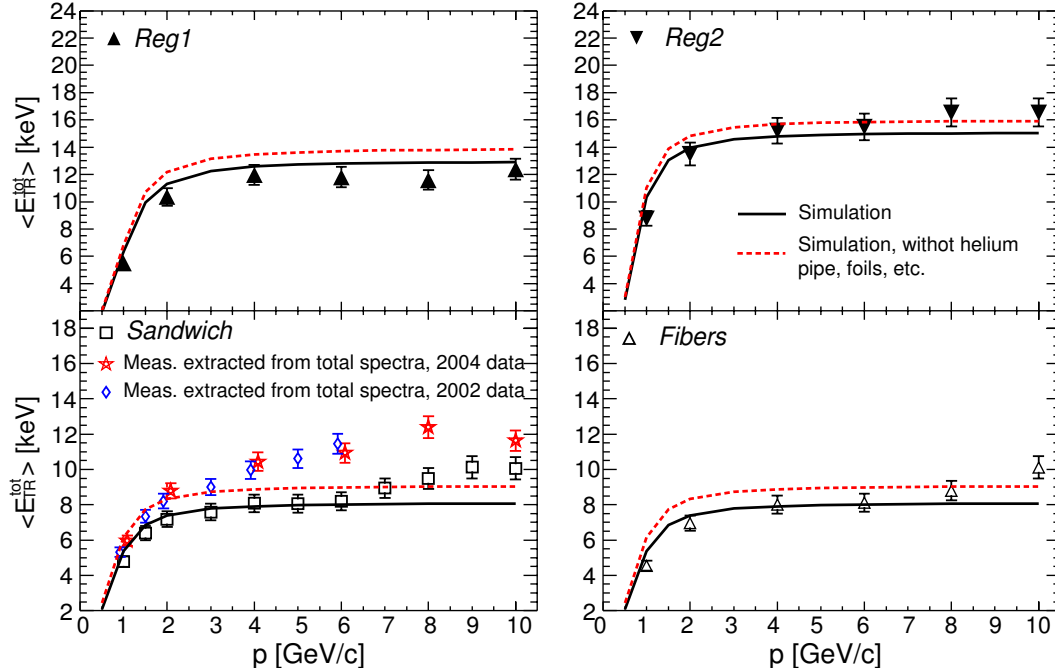
Fig. 14. Measured and simulated total TR energy $\langle E_{TR}^{tot} \rangle = \langle E_{TR} \rangle \langle N_{TR} \rangle$ as a function of momentum for the two regular foil radiators and for the *sandwich* and *fiber* radiators. For the *sandwich* radiator we also include mean values extracted from the total energy loss spectra.

Fig. 14 shows the momentum dependence of the mean total TR energy for the four radiators. In case of the *sandwich* radiator this observable can also be extracted from two measurements of total energy loss spectra in the drift chamber without radiators (only dE/dx) and with radiators (dE/dx + TR). In this case the energy spectra are averaged over four (2002) and three chambers (2004). The direct TR measurements are in general well reproduced by the simulations, but for the *Reg2*, *sandwich* and *fiber* radiator for momenta larger than 6 GeV/c the measured data points diverge from the saturated behavior predicted by the simulations. This is probably a systematic error connected with an underestimation of the SR background for higher momenta (Compare to Fig. 9). For the indirect measurement one expects a larger value for the total TR energy, due to the absorption of part of the TR in the helium pipe, etc. This is found also in the data at momenta up to 3 GeV/c, but at higher momenta the data shows no saturation and diverges from the prediction. The reason for this discrepancy is not understood in detail yet, but it certainly is of importance for a thorough understanding of the pion efficiencies achieved with the ALICE TRD. An observed layer dependence of this effect points at TR buildup and/or bremsstrahlung from the different detector layers.
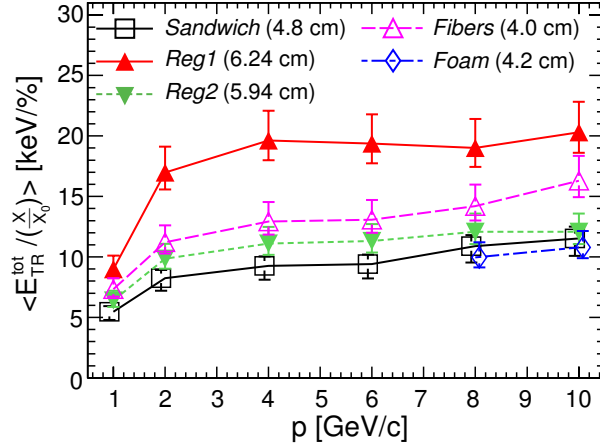
Fig. 15. Momentum dependence of the total TR yield of the different radiators scaled with their radiation length X/X_0.

4.7 Scaling with Radiation Length

In this section we investigate the mean total observed TR energy for the different radiators scaled with their radiation length: $\langle E_{TR}^{tot} \rangle / \frac{X}{X_0}$. The radiation length is a scaling variable for the probability of occurrence of bremsstrahlung and pair production, and for the variance of the angle of multiple scattering in the detector material. Since many transition radiation detectors are also used in experiments where track reconstruction of the particles is essential, a good TR performance should not be achieved at the expense of larger material budget. As we can see from Fig. 15, the good TR performance of the thicker regular radiator *Reg2* is achieved at the expense of about twice the radiation length; this is the reason why in this context the performance of *Reg2* is surpassed by *Reg1*. The *sandwich* radiator is not performing as well as the other radiators, which is due to the additional components used in its construction (carbon fiber coating, epoxy and aluminized mylar foil). In the case of the ALICE TRD, the radiators also serve the purpose of reinforcing the large area detectors against the gas overpressure, the weight of the Xe gas and the forces due to the sum of wire tensions. Due to the low radiation length, pure fibers – as used in ATLAS [20] – should be considered an attractive solution for tracking TRDs.

5 Summary and Conclusions

We have measured energy spectra of transition radiation (TR) for two regular foil and some irregular radiators (*fiber*, *foam*, *sandwich*) for electrons in the momentum range from 1 to 10 GeV/c with drift chambers operated with Xe, CO_2(15%). We used prototypes of the drift chambers to be used in the Transition Radiation

Detector (TRD) of the ALICE experiment at CERN.

We extracted cluster number distributions and found that they can be approximated by Poisson distributions. We observe a systematic increase of the measured photon yield as a function of momentum. This can be explained by synchrotron radiation, which is created by electrons in the magnetic field used to deflect the beam. The assumption that the increase of this photon background with momentum is due to synchrotron radiation is well explained by simulations. After subtracting this background, the mean values of the number of detected photons and of the total TR energy are essentially constant above 3 GeV/c.

The measured spectral shapes are quantitatively reproduced by simulations, in particular for the two regular foil radiators. For the *sandwich* and *fiber* radiators the simulation parameters only reflect typical dimensions of the radiator materials; we chose values that reproduce our data. With this method the momentum dependence of the mean TR energy deposit is quantitatively reproduced.

Our results significantly enhance the quantitative understanding of transition radiation; this is in particular the case for the performance of the *sandwich* radiators which are adopted in the ALICE TRD.

Acknowledgements

References

[1]   ALICE Transition Radiation Detector Technical Design Report, ALICE TDR 9, CERN/LHCC 2001-021.

[2]   C. Adler et al., Nucl. Instr. Meth. Phys. Res. A: 540 (2005), 140.

[3]   A. Andronic et al., Nucl. Instr. Meth. Phys. Res. A 498 (2003) 143.

[4]   A. Andronic et al., Nucl. Instr. Meth. Phys. Res. A 523 (2004), 302.

[5]   B. Dolgoshein, Nucl. Instr. Meth. Phys. Res. A 326 (1993) 434.

[6] A. Andronic et al., Nucl. Instr. Meth. Phys. Res. A 522 (2004) 40.

[7] A. Andronic et al., Nucl. Instr. Meth. Phys. Res. A 519 (2004) 508.

[8] O. Busch et al., Nucl. Instr. Meth. Phys. Res. A 522 (2004) 45.

[9] C.W. Fabjan and W. Struczinski, Phys. Lett. B 57 (1975) 483.

[10] M.L. Cherry at al., Phys. Rev. D10 (1974) 3594.

[11] M.L. Cherry at al., Phys. Rev. Lett 38 (1977) 5.

[12] A. Andronic et al., Nucl. Instr. Meth. Phys. Res. A 525 (2004) 447.

[13] R. Brun et al., Nucl. Instr. Meth. Phys. Res. A 502 (2003) 339.

[14] R. Brun et al., Geant 3 User Guide, CERN, 1985.

[15] S. Agostinelli et al., Nucl. Instr. Meth. Phys. Res. A 506 (2003) 250.

[16] A.Fassò et al., "Electron-photon transport in FLUKA: status", Proceedings of the MonteCarlo Conference, Lisbon, October 2000.

[17] S. Apostolakis et al., Comp. Phys. Comm. 132 (2000) 241; V.M. Grichine and S.S. Sadilov, Nucl. Instr. Meth. Phys. Res. A 522 (2004) 122.

[18] The Geant 4 collaboration, Physics Reference Manual, June 2005.

[19] Atomic and Nuclear Properties of Materials for 292 substances, http://pdg.lbl.gov/AtomicNuclearProperties/

[20] ATLAS Inner Detector Technical Design Report, ATLAS TDR 4, CERN/LHCC 1997-016.